Cylindrical phase of block copolymers: Stability of circular configuration to elliptical distortions and thin film morphologies

G. G. Pereira
Cavendish Laboratory, University of Cambridge, Madingley Road, Cambridge CB3 0HE, United Kingdom
(Received 13 November 2000; published 29 May 2001)

We study the cylindrical phase of a diblock copolymer melt in the strong segregation limit, and initially examine the stability of this morphology against elliptical perturbations. Surprisingly, we find that an elliptical conformation of the columns has lower free energy than a circular one. The size of the ellipse's eccentricity depends on *f*, the minority block fraction. We proceed to examine the morphology of the melt when placed between two hard, flat surfaces. The columns can either form with their axes in the plane of the bounding surfaces (denoted parallel) or with their axes perpendicular to the bounding surfaces. We determine when the parallel alignment is preferred over the perpendicular alignment.

DOI: 10.1103/PhysRevE.63.061809 PACS number(s): 61.41.+e, 68.03.Cd, 68.60.−p

Diblock copolymers (DCP) are made up of two chemically different polymer chains, denoted by *A* and *B*, joined together end to end. The self-assembly of the diblocks is driven by the immiscibility of the *A* and *B* components leading to microphase separation into a variety of morphologies with characteristic size of order 1000 Å . Some typical morphologies that form are lamellae, cylindrical, and spherical phases [1]. Here we concentrate on the case of an asymmetric DCP melt that forms a hexagonally packed cylindrical phase in the bulk. This has been shown to form (and seen experimentally) at a fraction of *A* monomers, denoted by *f*, between 0.12 and 0.29 [1]. We consider chains with degree of polymerization *N* and identical monomer size *a*. This morphology attempts to minimize the free energy of the system that is a sum of *AB* interfacial energy and elastic stretching energy of the chains.

It has now been recognized that the nanoscale morphologies produced by these self-assembling DCP melts may be used as lithographic templates for producing patterns orders of magnitude smaller than at present. Such reduction in scales may have huge benefits in device miniaturization. For example, Ref. [2] has focused on aligning thin films of the cylindrical phase of DCP melts with electric fields. There the DCP melt is placed between two oppositely charged, flat surfaces and the electric field enhances the columns to orient perpendicularly to the surfaces. Our work is, in part, motivated by such experiments but we focus on a more fundamental problem: the equilibrium, thin film morphology without external fields. The system becomes strained when a thickness is imposed on the film and together with the surface interfacial tension effects can deform the circular cross section of the columns.

There has been some theoretical work on thin films of the cylindrical phase of DCP melts [3–6]. However, they have concentrated mainly on the scenario where the surface energy favors one phase sufficiently, such that the cylindrical morphology is destroyed adjacent to the bounding surfaces. Instead a lamellar morphology forms there. Here we consider a slightly different scenario: the columnar morphology remains, but is allowed to be distorted. According to Turner *et al* [4] this may occur when $0<\gamma_{SB}-\gamma_{SA}<\gamma_{AB}$ where γ_{AB} is the *AB* interfacial tension and γ_{SB} is the surface-*B* phase interfacial tension, etc. We assume here the *A* (inner core) phase is preferred at the surface, so that the cylinders would prefer to align with their axis in the plane of the bounding surfaces (called parallel alignment from now on). This can be seen from Fig. 1 if one notes that in a parallel alignment the fraction of the surface covered by *A* monomers is $(2\sqrt{3}/\pi)^{1/2}\sqrt{f}$ while in perpendicular alignment it is only *f*. For example, at an *f* of 0.25 this implies in parallel alignment the fraction of the surface covered by *A* monomers is 0.52 while in perpendicular alignment it is only 0.25.

There is another motivation for our study. The self-assembled morphologies that form are, mathematically, minimal surfaces. They represent the minimal surface area for a given volume and so minimize the *AB* interfacial part of the free energy. However, it is not clear that the stretching energy is also minimized. In fact, what is done theoretically is that a number of possible structures is assumed, commonly the minimal surfaces such as spheres, columns and lamellae, and one compares the free energy of these phases to determine which one is actually observed. Therefore we test the stability of the circular cross section of the columnar phase to elliptical perturbations. Rather interestingly we find an elliptical cross section is slightly more stable than a circular cross section. In turn this leads to an asymmetric behavior

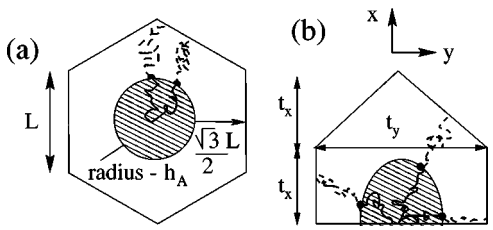

FIG. 1. Schematic of hexagonal phase showing columns (shaded circle of radius h_A) and matrix, with some ''typical'' chains. Dots represent the point where *A* and *B* chains are tethered together. (a) Perpendicular alignment (bounding surface in plane of paper). (b) Top half of the Wigner-Seitz cell on which our calculations are based. (Bottom half is mirror image of top half.) It consists of a hexagon (which can be deformed). The semimajor axis length of the ellipse (shaded area) is h_x, while the semiminor axis length is h_y.

depending on whether the system is expanded or compressed in the thin-film geometry.

We shall consider the strong segregation limit (SSL), where the interface between A and B regions is well defined and narrow and thus use Semenov's theory [7]. Although this theory has some well-known deficiencies, such as the exclusion zone that yields an underestimate of the free energy, it has one major advantage over other more accurate self-consistent field theories (SCFT) [8]. It allows us to pick any general shape for the AB interface, whereas the more accurate theories are currently limited to circularly symmetric structures. We shall discuss the validity of the results in the context of the approximations later. If we are deep in the SSL, i.e., γ_{AB} is large, then Turner's condition implies that the elliptic distortion considered here may occur for quite large surface interfacial tensions.

Let us consider first how to determine the minimum free energy of a bulk sample of this phase. This phase consists of columns of the A phase (minority phase) in a matrix of the B phase (majority phase). The discussion is based on arguments put forward by Semenov [7] and Likhtman and Semeron [9]. The elastic energy of the inner and outer domains of diblock chains, i.e., chains in the A and B regions, is given by

$$F_{el,i}=k_BT\frac{\pi^2}{16}\frac{1}{N_i^2a^2v}\int_{[i]}s^2(\mathbf{r})d^3\mathbf{r}, \tag{1}$$

where i can be either A or B, v the monomer volume, and N_i the number of monomers in the ith block. Here $s(\mathbf{r})$ is defined as the shortest distance from a given point to the nearest interface and the integration is performed over the volume of the ith domain. Figure 1(a) represents the bulk, circular symmetric case.

The elastic energy of the chains in the inner (A) domain (per chain) is quite simple: the limit of the cylindrical part of the integral in Eq. (1) is h_A, thus $F_{el,A}=k_BT\alpha_Ah_A^2/(Na^2)$ with $\alpha_A=\pi^2/(96f)$. The outer block's elastic energy is more tedious to calculate, since the domain of the B blocks does not have circular symmetry. To compute the outer domain's elastic energy one requires L in terms of h_A. This is obtained by using the volume constraint of A and B domains. Doing this one finds $L=[2\pi/(3\sqrt{3}f)]^{1/2}h_A$. After some algebra one can show that the elastic energy of the B domain (per chain) is $F_{el,B}=k_BT\alpha_Bh_A^2/(Na^2)$, where

$$\alpha_B=\frac{\pi^2}{16f(1-f)^2}\left[\frac{5\pi}{18\sqrt{3}}-\frac{4}{3}\sqrt{\frac{\sqrt{3}\pi f}{2}}\left(\frac{1}{3}+\frac{1}{4}\ln 3\right)+f-\frac{f^2}{6}\right]. \tag{2}$$

The interfacial AB energy (per chain) is simply $F_{AB}=2fNv\gamma_{AB}/h_A$, where γ_{AB} is the AB interfacial tension. The total energy is $F=F_{AB}+F_{el,A}+F_{el,B}$, which is minimized with respect to h_A to obtain the optimal radius of the columns. Carrying out the minimization yields the optimal radius

$$h_A^*=(\gamma_{AB}a^2/k_BT)^{1/3}N^{2/3}v^{1/3}[f/(\alpha_A+\alpha_B)]^{1/3} \tag{3}$$

and the corresponding minimum free energy is

$$F^*=3k_BT(v^{1/3}/a)^2N^{1/3}(\gamma_{AB}a^2/k_BT)^{2/3}f^{2/3}(\alpha_A+\alpha_B)^{1/3}. \tag{4}$$

The equilibrium center-to-center separation between columns, D_0, is $D_0=(2\pi/\sqrt{3}f)^{1/2}h_A^*$.

The above analysis has been carried out under the assumption that the cross section of the columns is circular and so the hexagon has six equal sides. We now relax this assumption and allow for the possibility of an anisotropic shape, see Fig. 1(b), with columns of elliptic cross section. Thus we have $h_x\neq h_y$ and so we define the eccentricity of the ellipse as $e=\sqrt{1-(h_y/h_x)^2}$, where the ellipse is extended in the x direction (or the top corner of the hexagon), see Fig. 1(b). We argue that the ellipse semimajor axis can only point in the direction of the hexagon's corner. The lengths t_x and t_y, shown in Fig. 1(b), are related to h_x and h_y by $h_x=3t_x(2f/\sqrt{3}\pi)^{1/2}$ and $h_y=t_y(\sqrt{3}f/2\pi)^{1/2}$. The distance from the center of the ellipse to the perimeter becomes angle dependent and is given by

$$h_A(e^2,\theta)=h_x(1-e^2)^{1/2}(1-e^2\cos^2\theta)^{-1/2},$$
$$\text{where}\quad 0<\theta<\pi/2. \tag{5}$$

We consider first the interfacial AB energy, which is essentially determined by evaluating the perimeter of an ellipse. The perimeter of the ellipse is just $4h_x(1-e^2)^{1/2}E(e^2/(e^2-1))$, where E is an elliptic integral of the second kind. The area of the ellipse is $\pi h_x^2(1-e^2)^{1/2}$ and so the interfacial (AB) free energy (per chain) is

$$F_{AB}=\frac{2F^*}{3}\left(\frac{h_A^*}{h_x}\right)\frac{2}{\pi}E(e^2/(e^2-1)). \tag{6}$$

The elastic stretching energy is more complicated to calculate than in the circular case because one must find a suitable minimal distance between the point to the AB interface. Let us consider some point with coordinates (r,θ). The distance from this point to any point on the AB interface is given by $s^2(\mathbf{r})=r^2+h_A^2(e^2,\phi)-2rh_A(e^2,\phi)\cos(\phi-\theta)$. This distance must be minimized with respect to ϕ, to give a $s_{\min}^2(r,\theta)$. This is then substituted into Eq. (1) and integrated. This results in elastic energies of

$$F_{el,i}=\frac{F^*}{3}\left(\frac{\alpha_i}{\alpha_A+\alpha_B}\right)\left(\frac{h_x}{h_A^*}\right)^2I_{el,i}, \tag{7}$$

where i is either the A or B domain. The important quantities are the integrals $I_{el,i}$. $I_{el,A}$ is given by

$$I_{el,A}=\frac{24}{\pi}(1-e^2)^{-1/2}\int_0^{\pi/2}d\theta\int_0^t d\tau\tau\zeta_{\min}^2(\tau,\theta,e^2). \tag{8}$$

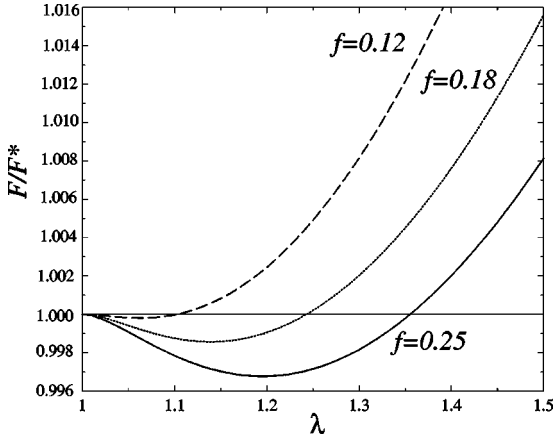

FIG. 2. Free energy of DCP melt as a function of λ for $f=0.25$ (solid line), $f=0.18$ (dotted line) and $f=0.12$ (dashed line).

$I_{el,B}$ is given by

$$I_{el,B}=\frac{\pi f(1-e^2)^{-1/2}}{4(1-f)^2\alpha_B}\left[\int_0^{\psi}d\theta\int_t^{\eta}d\tau\tau\zeta^2_{\min}(\tau,\theta,e^2)+\int_{\psi}^{\pi/2}d\theta\int_t^{\sqrt{1-e^2}r_t/\sin\theta}d\tau\tau\zeta^2_{\min}(\tau,\theta,e^2)\right], \quad (9)$$

where

$$\psi=\pi/2-\arctan[1/\sqrt{3(1-e^2)}],$$

$$r_t=(\pi/2\sqrt{3}f)^{1/2},$$

$$t=[(1-e^2)/(1-e^2\cos^2\theta)]^{1/2},$$

$$\eta=(2r_t/\sqrt{3})[\sin\theta/\{\sqrt{3(1-e^2)}\}+\cos\theta]^{-1},$$

$$\zeta^2_{\min}(\tau,\theta,e^2)=\tau^2-2\tau\cos(\phi_0-\theta)\frac{(1-e^2)^{1/2}}{(1-e^2\cos^2\phi_0)^{1/2}}+\frac{(1-e^2)}{(1-e^2\cos^2\phi_0)} \quad (10)$$

and $\phi_0(\tau,\theta,e^2)$ is the optimal value of ϕ that minimizes ζ^2. Note that the integrals $I_{el,A}$ and $I_{el,B}$ are just functions of e. The energy, per chain, is then $\mathcal{F}=F_{AB}+F_{el,A}+F_{el,B}$. For given h_x, $\mathcal{F}$ must be minimized over e to obtain the minimum free energy and hence the optimal relaxation in the orthogonal direction.

Figure 2 shows the scaled free energy $\mathcal{F}/F^*$ as a function of $\lambda\equiv h_x/h_A^*$. At $\lambda=1$, the optimal state is $h_x=h_y=h_A^*$ with a free energy F^*, which is Semenov's result [9]. The results are shown for three A monomer fractions, $f=0.12$, 0.18, and 0.25. There are a number of very interesting features about the free energy plots. Firstly, the minima are not at $\lambda=1$, but at $\lambda=1+\epsilon_x(f)$ with $\epsilon_x(0.25)\approx0.20$, $\epsilon_x(0.18)\approx0.12$, and $\epsilon_x(0.12)\approx0.06$. In turn, the center-to-center column spacing in the x and y directions, which in the pure circular case are related by $D_{0x}/\sqrt{3}=D_{0y}=D_0$, become $D_{0x}=\sqrt{3}D_0[1+\epsilon_x(f)]$ and $D_{0y}=D_0[1-\epsilon_y(f)]$, where $\epsilon_y(0.25)\approx0.13$, $\epsilon_y(0.18)\approx0.09$ and $\epsilon_y(0.12)\approx0.05$. Thus the elliptic configuration is actually a lower energy state than the circular configuration. In general we write the free energy as $F_{\min}(f)=[1-\delta(f)]F^*$ and so $\delta(0.25)\approx0.00322$, $\delta(0.18)\approx0.00125$, and $\delta(0.12)\approx0.00019$. It can be seen that for larger f the cross section is more eccentric. This is readily explained since for large f the system tends to become more elongated (goes to a lamella structure) while for small f it becomes more circular (goes to a spherical structure). Figure 2 implies that the circular cross section is unstable to elliptical perturbations. However, because of the approximate nature of Semenov's theory and the small differences between the circular and elliptic conformations, further, more accurate calculations such as SCFT [8] or advanced SSL [9] need to be carried out to confirm the result.

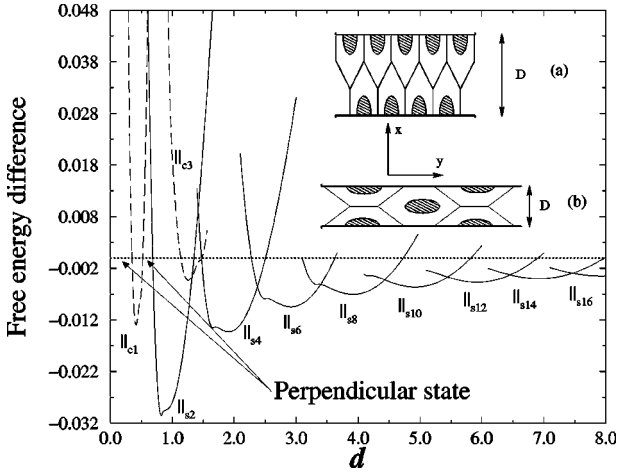

FIG. 3. Free energy difference plotted as a function of scaled film thickness $d\equiv D/(D_{0x}/2)$ for $\Delta\gamma\equiv(\gamma_{SB}-\gamma_{SA})/\gamma_{AB}=0.15$ and $f=0.25$. Dashed curves are $\|_c$, while solid curves are the $\|_s$. The numbers relate to the number of layers. First order transitions occur at intersection of curves. In the inset we show schematically (a) the $\|_{s2}$ orientation while in (b) the $\|_{c2}$ orientation.

We now proceed to determine the thin-film morphology of this DCP melt. The additional free energy term is a surface energy contribution due to the presence of bounding surfaces. In parallel alignment of the columns, the column axes are considered to align with the z axis, while in perpendicular alignment the column axes align with the x axis. The surfaces that bound the sample are in the y-z plane, orthogonal to the x axis. There are two possible orientations in parallel alignment, see Fig. 3, where in (a) the film is stretched, denoted $\|_s$ from now on, while in (b) it is compressed, denoted $\|_c$. We consider thin films in a rectangular space, i.e., D units in the x direction, L_y units in the y direction and L_z units in the z direction. We assume that the ellipses adjacent to the surfaces have the same shape and dimensions as those in the interior. In this way any strain is shared equally between the layers as the film thickness is varied, in analogy with thin-film lamella problems [10]. Half ellipses must form adjacent to the surfaces, so that the chain trajectories are not impeded by the surfaces and consequently the hexagonal structure is not lost.

In the $\|_s$ case, $t_x=2D/(3\rho)$ where ρ is the number of

layers in the x direction, $\rho=2,4,6,\ldots$. In the $\|_c$ case the number of layers may be even or odd so that $t_y=2D/\rho$ where $\rho=1,2,3,\ldots$. Since the ratios h_y/t_y and h_x/t_x are constants, the surface energies do not change when a deformation occurs as one would expect since volume must be conserved. To determine the surface energies we must simply determine the difference in the fraction of A monomers at the surface between the two alignments. The surface energy difference (per chain) between the various alignments are $F_{surf,\|_s}-F_{surf,\perp}=-2(Nv/D)[(2\sqrt{3}f/\pi)^{1/2}-f]\times(\gamma_{SB}-\gamma_{SA})<0$ and $F_{surf,\|_c}-F_{surf,\perp}=-2(Nv/D)\times[(2f/\sqrt{3}\pi)^{1/2}-f](\gamma_{SB}-\gamma_{SA})<0$. Since we assume $\gamma_{SB}-\gamma_{SA}>0$, the $\|_s$ state will be preferred to the $\|_c$ state on surface energy considerations. The free energy difference between $\|_s$ and $\perp$ states (ΔF_1) and $\|_c$ and $\perp$ states (ΔF_2) are now obtained by adding the bulk energy term, $\mathcal{F}$ (outlined above), which is now dependent on the film thickness, D. If the $\|_s$ (or $\|_c$) state is compressed below $D_{0x}/2$ (expanded above $D_{0y}/2$), we assume that the Wigner-Seitz cell compresses (expands) uniformly in all directions.

The free energy difference between the parallel and perpendicular alignments is shown in Fig. 3 for $f=0.25$ and $\Delta\gamma\equiv(\gamma_{SB}-\gamma_{SA})/\gamma_{AB}=0.15$. When $\Delta F_i<0$ $(i=1,2)$ the parallel states are observed and when the converse is true the perpendicular state is observed. The surface term scales like D^{-1} and so its effect is most significant for thin films, as one would expect. The free energy has the characteristic ''discrete'' shape for a layered system [10]. Minima are slightly shifted off integer values due to the surface contribution. The $\|_s$ state is seen predominantly, since this state has the most favorable surface energy contribution. The $\|_c$ is seen at relatively thin films, while for the thinnest films the systems reverts to a perpendicular configuration, as expected. Note that only the odd $\|_c$ states are seen. The even $\|_c$ states have their minima close to the $\|_s$ state minima but because of the unfavorable surface energy contribution for this orientation, in comparison to $\|_s$, the $\|_s$ state is preferred. Qualitatively, these columnar systems behave analogously to lamellar systems [10], with transitions from n to $n+1$ layers $(n=1,2,\ldots)$ as the film thickness increases. Kinks in the free energy curves are due to the columnar cross sections changing from circular to elliptical configurations.

In conclusion we have, for the first time, considered the stability of the circular cross section of the hexagonal phase of an asymmetrical DCP melt in the SSL. Although our theory is approximate, it shows that this configuration is unstable to small elliptical perturbations. Further, more accurate SSL theories [9], will be applied to confirm the result. As well, we hope this work will stimulate SCFT [8] calculations for this configuration. It has been seen for large f that the elliptical distortion can be quite large, up to $e^2\approx0.48$, however, the energy well of this minima is quite shallow and broad. As such, it might be that thermal fluctuations could mask a clear observation of the distortion. The physics behind the elliptic distortion is apparent—although the surface tension favors a minimal surface (i.e., circular cross section) the elastic stretching term favors an elongated structure and the best compromise is an elliptic distortion. We have also calculated the thin-film morphology in the case where $0<\Delta\gamma<1$. The thin-film analysis is not as delicate as the stability analysis, since it can be readily shown that when strain is imposed on these thin films an elliptical morphology has a significantly lower free energy than a circular one. We have found that as the film thickness varies, the cross sections of the columns become increasingly elliptical.

I acknowledge useful discussions and clarifications with M. Warner and A. N. Semenov, and support from the EPSRC.

[1] F. S. Bates and G. H. Fredrickson, Annu. Rev. Phys. Chem. **41**, 525 (1990); Annu. Rev. Mater. Sci. **26**, 501 (1996).
[2] T. Thurn-Albrecht *et al.*, Science **290**, 2126 (2000); T. Thurn-Albrecht *et al.*, Macromolecules **33**, 3250 (2000).
[3] G. Brown and A. Chakrabarti, J. Chem. Phys. **101**, 3310 (1994).
[4] M. S. Turner, M. Rubenstein, and C. M. Marques, Macromolecules **27**, 4986 (1994).
[5] K. Y. Suh, Y. S. Kim, and H. H. Lee, J. Chem. Phys. **108**, 1253 (1998).
[6] H. P. Huinink, J. C. M. Brokken-Zijp, and M. A. van Dijk, J. Chem. Phys. **112**, 2452 (2000).
[7] A. N. Semenov, Zh. Eksp. Teor. Fiz. **88**, 1242 (1985) [Sov. Phys. JETP **61**, 733 (1985)].
[8] M. W. Matsen and M. Schick, Phys. Rev. Lett. **72**, 2660 (1994).
[9] A. E. Likhtman and A. N. Semenov, Macromolecules **27**, 3103 (1994); Europhys. Lett. **51**, 307 (2000).
[10] M. S. Turner, Phys. Rev. Lett. **69**, 1788 (1992); D. G. Walton *et al.*, Macromolecules **27**, 6225 (1994).